Crack propagation resistance of TiAl alloys

R. Pippan and A. Hohenwarter*

In their temperature window of application, TiAl alloys typically fail in a semi-brittle manner. For this material class, the Griffith concept, developed initially for ideal brittle materials, has to be adapted by additional dissipative contributions to the fracture resistance: plastic deformation, crack bridging, the work to deform and fracture shear ledges, and crack bifurcation. These additional terms in the fracture resistance induce a pronounced R-curve effect or in other words, a crack extension-dependent fracture resistance for monotonic and cyclic loading. In order to deliver guidelines to optimize the microstructural design and to enhance the fracture resistance of TiAl alloys, model systems, including a polysynthetically twinned TiAl, a designed fully lamellar and a near-gamma TiAl alloy are discussed in terms of their fracture mechanism using the energy and stress intensity approach.

Introduction

For crack propagation, if only the work of separation between the atoms is required, the fracture behavior is called ideal brittle fracture. Griffith[1] has introduced an energy approach to describe this type of failure. However, this type of fracture is quite rare; silicon single crystals fail typically by this kind of failure. There is a vast number of materials, including various structural materials that fail by a cleavage fracture mode where also the breaking of the atomic bonds determines the intrinsic failure process. However, in that case, besides the work of separation of the atomic bonds, various additional dissipative processes occur. All bcc metals and alloys fail by this fracture mechanism below a certain critical temperature. Also in most intermetallic compounds, crack propagation takes place in a semi-brittle manner at low and medium temperatures, sometimes denoted as quasi-brittle mode.

In this article, a closer look at the specific phenomena of crack propagation of interesting TiAl alloys is presented. This contribution is not meant to be a review of fracture toughness and fatigue crack propagation of TiAl alloys; for this purpose, please see example.[2–8] The goal is to illustrate the fracture processes and try to show how the extension of the Griffith concept by Orowan[9] and Irwin[10] can be used or extended to describe the resistance against crack growth.

First, a short introduction to various microstructures that can be generated in technically relevant compositions is given. Then, the fracture process in three model systems, a polysynthetically twinned TiAl, a designed fully lamellar (DFL), and a near-gamma TiAl alloy in fracture toughness experiments is presented, whereby the latter two can be considered as extreme variants of the technically used variants. The resulting R-curves for the crack growth resistance are discussed in terms of both the energy and stress intensity approach. Finally, significant microstructural parameters influencing the fracture resistance are considered on the base of the different toughening mechanisms.

Remarks to the microstructure of engineering relevant TiAl alloys

TiAl alloys with 42–49% Al and small additions of other alloying elements (Nb, Mo, B) are important for technical application due to their exceptional specific strength in the temperature window from 500 to 750°C. The multifarious phase features in the temperature window between 1100 and 1500°C permit the generation of a large variety of microstructures. A

R. Pippan, Erich Schmid Institute of Materials Science, Austrian Academy of Sciences, Leoben, Austria; reinhard.pippan@oeaw.ac.at
A. Hohenwarter, Department of Materials Science, Chair of Materials Physics, Montanuniversität Leoben, Leoben, Austria; anton.hohenwarter@unileoben.ac.at
*Corresponding author
doi:10.1557/s43577-022-00387-2

short description of the technically interesting TiAl alloys is given in the following.

Designed fully lamellar alloys consisting of γ-TiAl and α_2-Ti_3Al lamellae are one extreme version. The γ-TiAl has an ordered face-centered tetragonal L_{10} crystal structure, whereas the α_2-Ti_3Al phase has an ordered hexagonal DO_{19} crystal structure. The ratio of α_2/γ lamellae is typically about 1:10 or somewhat smaller. In contrast to the α_2 lamellae, which are essentially homogeneous, the γ lamellae consist of different domains, separated by twin boundaries. In a designed fully lamellar microstructure, the lamellae colonies form a dense structure. The size of the colonies of the investigated microstructures varies between 10 and several 100 µm. Also, the spacing of the lamellae can differ between few 10 nm and about 1 µm and controls the strength and creep resistance.

In contrast, the near-gamma microstructure represents the other extreme of the TiAl microstructures. It consists of polycrystalline γ grains with small percentages of α_2 phases at the grain boundaries and their triple junctions. The grain size of the investigated near-gamma microstructure is typically few 10 µm. Duplex microstructures are combinations of these two microstructures, consisting of a composite structure of gamma grains and α_2/γ lamella colonies.

The most technically used TiAl alloys are nearly fully lamellar microstructures with about 80–95% fully lamellar colonies surrounded by a variety of phases and different arrangement among them, which should guarantee a certain ductility of the usually brittle fully lamellar microstructure.[11,12]

Description of the fracture behavior of TiAl alloys

One "extreme" case of the fracture behavior of lamellar structures can be showcased with polysynthetically twinned (PST) crystals,[13] which allow us to conveniently study the effect of the loading direction and orientation of the lamellar structure on the fracture toughness. The fracture toughness in such a structure is strongly dependent on the lamella orientation (see **Figure 1**). When the pre-crack is introduced parallel to the lamellar structure (Figure 1a), the material behaves almost ideal brittle (Figure 1b). In contrast, when the pre-crack is perpendicular to the lamellae, the fracture toughness is dramatically enhanced. That means the fracture behavior is strongly anisotropic, where the crack propagates with low resistance parallel to the lamellae (Type A) and much higher resistance when the crack has to propagate across the lamellar boundaries (Type B).

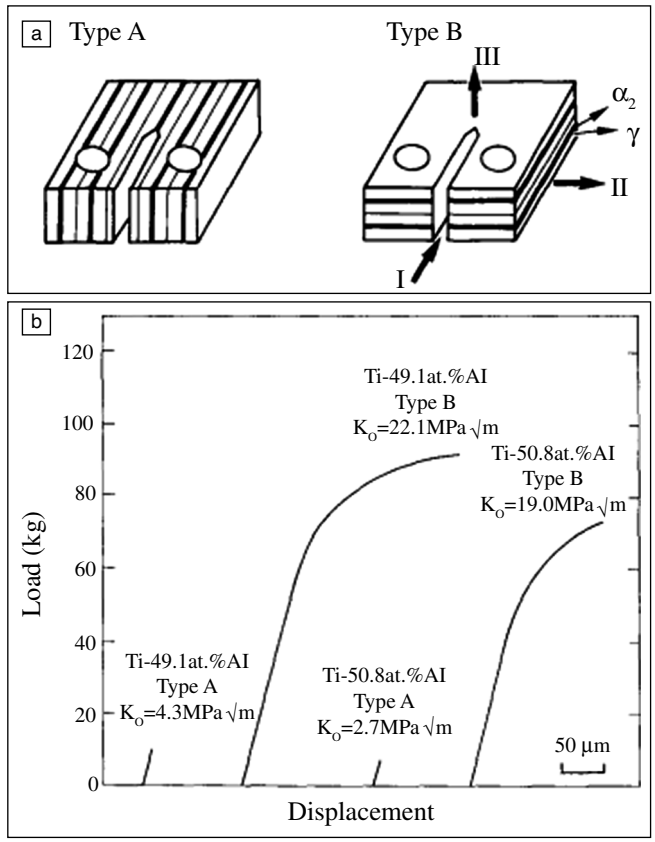

Figure 1. Fracture of polysynthetically twinned TiAl.[13] (a) Different specimen orientations in the short transverse (Type A) and crack divider (Type B) orientation. (b) Typical load–displacement curves for the orientations with slightly different Al contents.

From the technical point, more important is the crack propagation behavior of a designed fully lamellar microstructure (DFL). Important fracture features of a DFL microstructure are summarized in **Figure 2**. The colony size of the investigated alloy is relatively coarse, about 200 µm. At very small stress intensities, between 5 and 12 $MPam^{1/2}$, blunting by dislocations or twinning of few 100 nm occurs (Figure 2a–d), followed by a first real cleavage-like crack extension of a few microns (Figure 2e). This first crack extension strongly depends on the local microstructural arrangement. At a stress intensity between 12 and 25 $MPam^{1/2}$, crack extensions of several 10 µm combined with stopping and blunting of a few 100 nm take place (Figure 2e–f). In the DFL microstructure, the length of deflected segments is rather long. The frequency of branches, the formation of microcracks, the formation of interconnected microcracks, and the bridges and shear ligaments allow a stable crack propagation at large stress intensities or in other words, lead to the formation of an R-curve (Figure 2g–h). It seems that microcracks generate in front of the crack; however, in most cases, these are tunneling cracks starting from the interior of the colonies that fail by cleavage and then approach the sample surface. This can be clearly seen from the fractographic SEM image of the corresponding sample shown in the same figure (Figure 2i). The identical position on the fracture surface (Figure 2i)

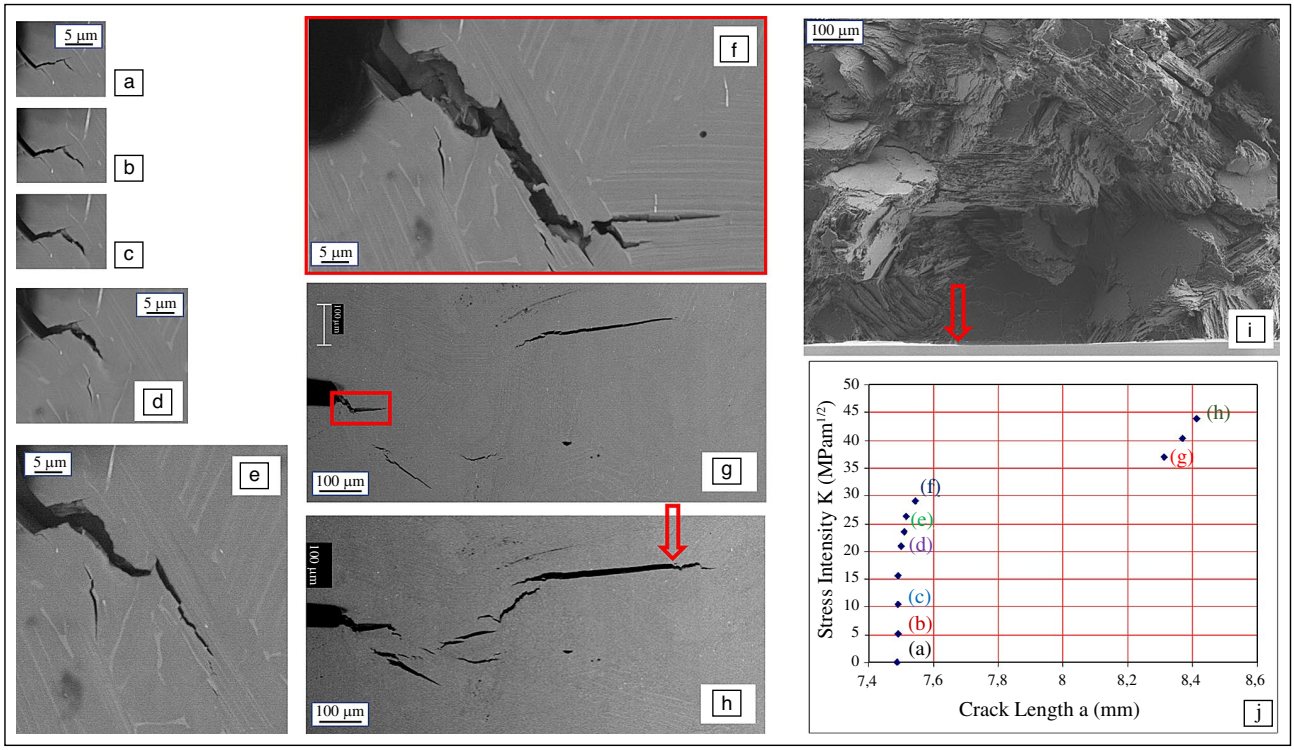

Figure 2. Fracture of designed fully lamellar microstructure;[14] please take into account the different scale in the scanning electron microscope (SEM) images. *In situ* crack growth experiment (a–h), as well as the corresponding fractograph (i) and resulting R-curve (j). Corresponding position in the SEM image (h) and the fractograph (i) are marked with a red arrow.

and the surface image (Figure 2h) are marked with a red arrow. The cleavage crack propagation of the large colonies in the interior of the sample and its tunneling to the surface is clearly visible. After building up the bridging zone of nearly 1 mm, which is about five times the colony size, the sample fails at a stress intensity of about 30 MPam$^{1/2}$. The corresponding R-curve is presented in Figure 2j. The cleavage of colonies occurs usually at the α_2/γ interface,[15] which seems to be the weakest cleavage plane.[16,17]

With increasing test temperature up to 600°C, the fracture initiation toughness increases somewhat, and at even higher temperatures a further pronounced increase of the initiation toughness can be seen (**Figure 3**). However, the R-curve at larger crack extensions, and therefore the maximum stress intensity, does not increase so intensively, indicating that the contribution of the bridge shielding mechanism is not significantly changed. At 800°C, the R-curve behavior is restricted due to a change to ductile fracture. However, even at this high temperature, few favorable aligned colonies fail in a quasi-cleavage mode. The remaining ligaments fail by delamination, necking of the ligaments, and finally by a micro-ductile failure. Important to note is the extreme scatter in the first section of the R-curve. This is mainly caused by the large colony size compared to the sample thickness (about 2 mm) in the investigated DFL microstructure.

Figure 4 illustrates the crack propagation behavior of a near-gamma alloy.[14] The very early fracture phenomena, where no large crack extension takes place, are similar to the DFL microstructure, blunting of few 100 nm combined with small cleavage crack extension (Figure 4a). For K-values larger than 9 MPam$^{1/2}$, the NG-structure develops only a flat R-curve of the fracture resistance, which is mainly induced by shear ligaments and the few crack bridges (see the *in situ* SEM micrographs in Figure 4b). The fracture surface remains quite flat (Figure 4c); on the mesoscale, it seems that it does not follow a specific crystallographic plane; however, on the very local scale, it seems that specific cleavage planes are preferred.[15] In principle, the fracture surface looks similar to typical polycrystalline bcc metals with a cleavage appearance of the fracture at low temperature. Contrary to the DFL microstructure, both the initiation fracture resistance as well as the R-curve contribution to the propagation resistance increase remarkably with temperature (Figure 4d).

Griffith approach versus stress approach

In order to describe the crack propagation condition of technically relevant structural materials, Orowan[9] and Irwin[10] have shown that the Griffith concept is also applicable to this group of materials; the essential change is the work to generate the fracture surfaces. In the framework of the Griffith concept,

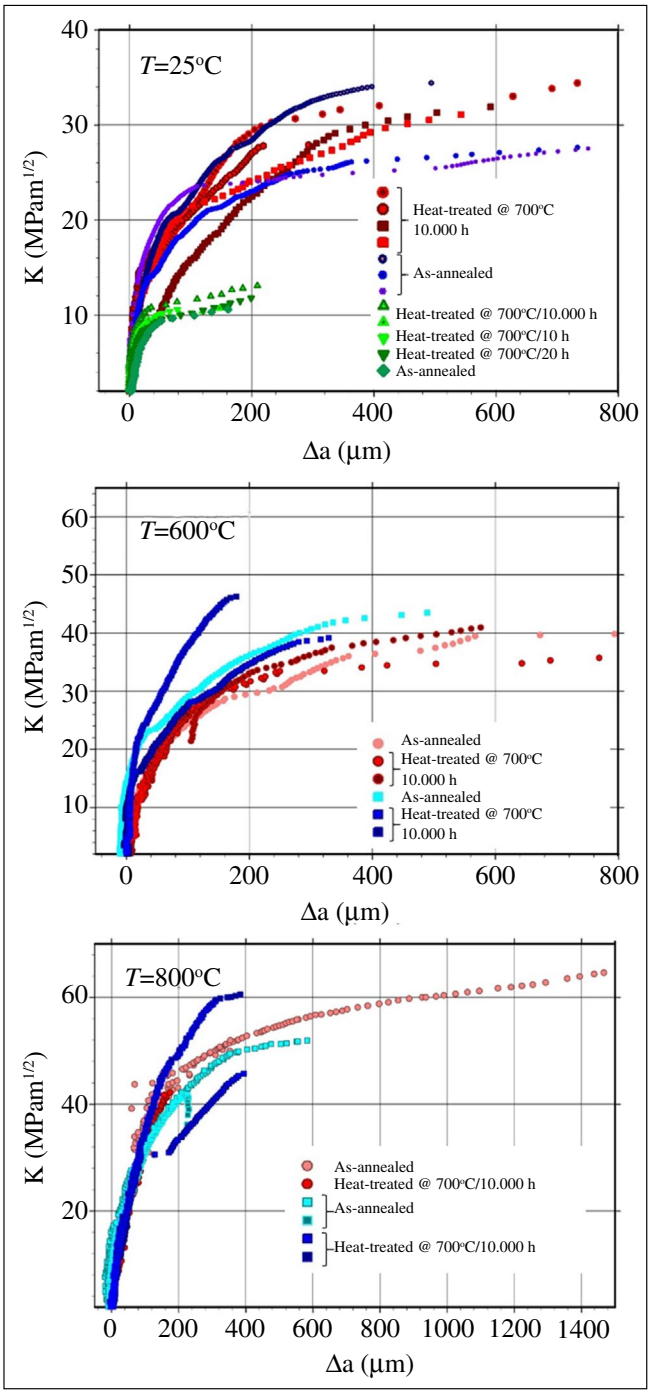

Figure 3. R-curves of fracture toughness of designed fully lamellar microstructure at room temperature (RT), 600°C, and 800°C. For RT, also the results in a fine-grained microstructure (green symbols) are indicated for comparison.[14] Note that the additional heat treatment (see symbols) does not alter the R-curve behavior distinctively.

which basically describes the criteria for crack propagation for ideal brittle materials, only the work of separation of the atomic bonds has to be spent, which is twice the surface energy, $2\gamma_s$. For ductile materials, the work necessary to form and move the plastic zone through the material has to be added. Hence, the crack growth resistance or critical energy release rate, G_{IC}, for ductile materials changes to

$$G_{IC} = 2(\gamma_s + \gamma_{pl}), \quad 1$$

where γ_{pl} is the plastic work per unit fracture area spent on one side of the growing crack. In more detail, γ_{pl} can be divided in a part necessary to form and move the plastic zone through the material, $\gamma_{pl\ z}$, and the plastic work required to form the dimples, $\gamma_{pl\ d}$ on the resulting fracture surface.[18] In ductile materials, the second part is usually small compared to the first one. As long as the plastic zone in front of the propagating crack is small compared to the size of the crack and ligament length, or in other words as long as small scale yielding prevails, the Griffith concept is applicable. A crack will propagate if the energy release rate is equal or larger than G_{IC}. G_{IC} is thereby a material constant as long as the sample thickness is large compared to the plastic zone, because under this condition, the plastic deformation in front of the crack is dominated by plane strain conditions. If this is not the case, the fracture resistance becomes thickness-dependent and can also develop an R-curve behavior.

In the case of semi-brittle materials, such as TiAl alloys, $\gamma_{pl\ d}$ vanishes except in the case of a mixed micro-ductile and cleavage fracture, which is the case for the designed fully lamellar microstructures at temperatures larger than 750°C (see Figures 2 and 3). In addition to γ_{pl}, the specific work to deform the crack bridges and shear ligaments, and finally to fracture these bridges, γ_{bf} has to be added. Hence, the fracture resistance, G_{IC}, can be written as

$$G_{IC(\Delta a)} = d_{(\Delta a)}\gamma_s + 2\gamma_{pl(\Delta a)} + \gamma_{bf(\Delta a)}, \quad 2$$

where $d_{(\Delta a)}$ is a factor larger than 2, which takes into account that the cracks, especially in the designed fully lamellar microstructures, exhibit very pronounced crack deflection, crack branching, and microcrack formation, resulting in a total fracture surface being significantly larger than the projected fracture surface. Except for the work of separation (equal to twice the surface energy, γ_s), which is an area weighted mean value of the work of separation of the cleavage planes of all different phases or interfaces of γ–γ or α–γ lamellae, and the interfaces to other phases, all other parameters increase with crack extension. Only for large crack extensions, the contributions reach a constant value that coincides with reaching the long crack fracture resistance. $d_{(\Delta a)}$ increases with crack extension by spreading of the crack front via crack deflection, crack branching, crack tunneling, and microcrack formation. γ_{pl} increases also due to the spreading of the crack front and increasing mode mixity at the crack tip. The increase of the specific work to deform the crack bridges and shear ligaments elastically and plastically

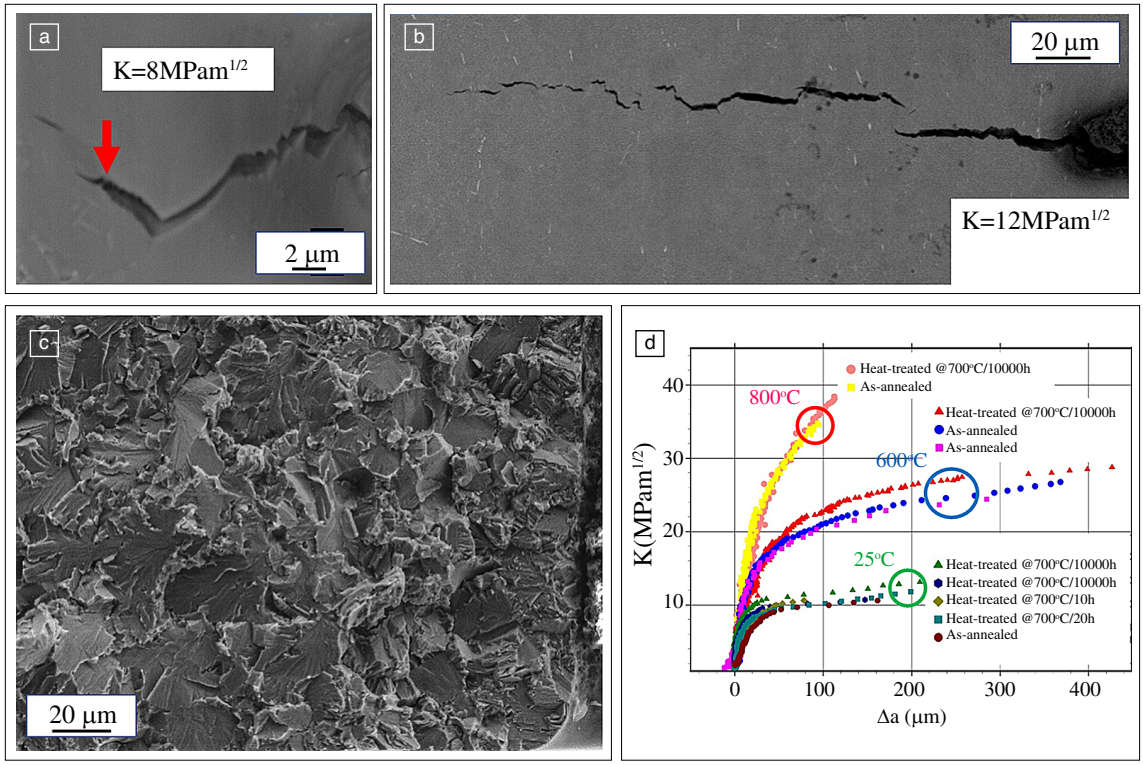

Figure 4. Fracture of a near-gamma microstructure, *in situ* scanning electron microscope images recorded at the onset of the R-curve (a, b); also the corresponding fractograph is shown for a room-temperature (RT) experiment (c). The R-curves for crack propagation at RT, 600°C, and 800°C are illustrated as well (d), where the crack extension was determined by the potential drop technique.[14]

and finally to fracture these bridges, γ_{bf} is quite evident if one looks to the fracture toughness as a function of crack extension depicted in Figures 2, 3, and 4, but also from the crack bridges seen in Figures 2 and 4. This value reaches a saturation when the number of generated crack bridges becomes equal to the number of fractured bridges. Despite this simple summation (Equation 2), a well-defined separation of the individual contribution is not straightforward or nearly impossible. The sum is measurable, but the determination of the specific increase of fracture resistance with crack extension (i.e., the R-curve) is a difficult task. The problem is the generation of a pre-crack free of these crack-length-dependent terms; this would require an atomistic sharp crack tip with a straight crack front and a plane fracture surface (i.e., a geometrically ideal crack). Furthermore, there exists no standard for the measurement of the R-curve for such semi-brittle materials. We use the following approach. We generate a very sharp notch by a razor blade polishing technique, which permits to generate notch root radii between 5 and 10 µm even in large specimens. Then, a pre-crack is generated with the smallest possible load in cyclic compression. In cyclic compression, the crack stops propagation after a certain number of load cycles[19] due to the sharp notch root and the low opening angle, and a pre-crack length of only somewhat larger than the notch root radius is necessary. Such pre-cracks are not ideal pre-cracks, but come very close to them. A further problem is the measurement of crack extension during the experiment due to the development of crack bridges and shear ligaments, which would not be accounted for by simple optical crack extension measurements. Hence, it is always necessary to clearly point out which technique for pre-cracking has been used and how the crack extension was measured.

Whereas the global behavior of the crack is well describable by this energy approach or the global K approach, the local criteria for crack propagation are somewhat easier to designate in the stress approach (i.e., in terms of the local stress intensity factor, k). A propagation of the crack by cleaving (separation of the atoms at the crack tip) the grains, lamellae, or the different types of interfaces occurs if the local stress intensity k is larger than the corresponding Griffith toughness K_G.

$$K_G = \sqrt{E \times 2\gamma_s/(1-\nu^2)}, \qquad 3$$

where $2\gamma_s$ is the corresponding work of separation of the atoms on the cleavage planes or the interfaces and v is the Poisson's ratio. The local stress intensity is given by the applied stress intensity range, K, plus the shielding and anti-shielding contributions,

$$k = \alpha K + \sum K_D + \sum K_T + \sum K_B. \qquad 4$$

It should be noted that due to the 3D shape of the crack, the local k is usually a mixed mode parameter, described by a mode I, II, and III component. The parameter α takes into account the geometric shielding due to the complex spreading of the crack by crack deflection, crack branching, and crack tunneling. For a 2D consideration of crack deflection and crack branching, the α parameters are well documented;[20] however, for the real complex 3D shape, as in the case of the designed fully lamellar microstructure, a simple estimation or approximation is not known to the knowledge of the authors and a numerical evaluation would be required. K_D and K_T are the shielding (negative values) and the anti-shielding (positive values) contributions of the dislocations and twins, respectively. The geometrical dependence of the K_D values for the 2D approach is again well documented.[21] For the K_T contribution, the same equation can be used by taking into account the collective effect of the partial dislocations forming the twin. However, for the actual 3D case, this analysis has not been performed yet. In the 3D case, a single dislocation can have a shielding in one region and an anti-shielding in another region. To the authors opinion this is one of the essential missing links to understand the semi-brittle crack propagation, not only in TiAl but also in many other materials. Finally, K_B is the shielding induced due to the load transfer through the crack bridges and shear ligaments; these forces always provide a shielding (i.e., a negative contribution). In contrary, K_D and K_T can be positive or negative, and even α can be smaller or larger than 1, only in the 2D case it is always below 1. Values for α larger than 1 are a consequence of the crack front curvature.

The mentioned mode mixity is not only a consequence of the crack deflection, the crack branching, and the complex shape of the crack front (i.e., the geometry). It is also changed by the plastic deformation, as the generated dislocations and twins induce not only a shielding or anti-shielding contribution, but they also change the mode mixity. The crack bridges and shear ligaments induce primarily a mode I shielding of the leading main crack front. The mode mixity of the remaining (micro-) cracks in the bridges and shear ligaments is determined by the geometry and the elastic and plastic deformation of these microfracture mechanical elements. Even for these microcracks, the propagation condition in a cleavage mode is still determined by the Griffith concept; however, the dislocation and twinning activity in these micro elements will change the local stress intensity and mode mixity. In addition, it should be noted that this local mode mixity will also change the competition between cleavage and dislocation or twin generation at the crack tip.

The Griffith concept has been developed for mode I loading. The question of a general transferability to mixed mode loading is in the authors opinion not solved yet. There is no doubt that cleavage crack propagation is mode I dominated, which is clearly visible from pure mode II loaded cracks, where the crack deflects and propagates always mode I dominated. However, for the local propagation condition, the question remains whether the local k_I component or the total local k must become larger than the Griffith toughness for crack propagation.

Despite a principle understanding of the crack propagation criteria, the prediction of the crack path is actually impossible, except for very simple microstructures such as the polysynthetically twinned TiAl. The reason for this is not only the complexity of the real crack shape embedded in the microstructure, but also the differences in the local cleavage resistance, γ_s, of the different cleavage planes and all kinds of interfaces. Therefore, it is not surprising that well-defined design criteria for optimizing the fracture toughness do not exist. Nevertheless, some hints for improvement of the fracture toughness can be derived from the previously described consideration founded on the energy as well as the stress approach. But for all optimization strategies, one has to clearly distinguish between the long crack fracture toughness and the R-curve behavior, as well as the need for which one should be optimized. In principle, for highly stressed components, a steep increase of the R-curve is beneficial, whereas for low stressed components, the long crack fracture toughness is more important.

Both the energy and the stress approach can be described by a linear sum (Equations 2 and 4), which is evident for the global energy balance. But also for the stresses, the description in Equation 4 assumes ideal linear elasticity and hence a linear sum is applicable. Plasticity in this approach is simply a consequence of the moving dislocations or partial dislocations of the twins in an ideal elastic material. The decohesion of the atomic bonds at the crack tip is like an ideal brittle material determined by the Griffith toughness, whereas the crack propagation is governed by the shielding and anti-shielding along the crack path. Despite these two simple sums (Equations 2 and 4), calculation of the energy contributions from the shielding contributions and vice versa is not straightforward. Only for the applied global and local K, k and G, G_{tip}, the simple relation $G = K^2/E(1 - \nu^2)$ holds, respectively. Calculation of the global values of γ_{pl} and γ_b from local shielding values is, however, not possible in such a simple form due to the different approaches and square relation between G and K.

Finally, it should be mentioned that the consideration of the fatigue crack propagation behavior in TiAl alloys is quite similar, because the crack propagation mechanism is predominately a cleavage process, which seems to be mainly governed by the cyclic loading-induced failure of the crack bridges and shear ligaments.[14,22]

Conclusion and some consequences for improving the crack growth resistance

Technically, relevant TiAl alloys exhibit a semi-brittle crack propagation behavior below 750°C, which is within the typical application window of this class of alloys. Hence, the fracture toughness below the ductile to brittle transition temperature is an essential material property for any safe design. In order to demonstrate the fracture processes and the large variation of the fracture resistance, the crack propagation behavior of a coarse-grained designed fully lamellar and a near-gamma TiAl alloy is presented. The crack growth resistance of all other technically relevant microstructures is usually a mixture of the fracture processes of these two extreme microstructures.

Contrary to the classical Griffith concept, an essential feature of these semi-brittle materials is the R-curve behavior of the crack propagation resistance, which can be described by an increase of the critical energy release rate or the critical stress intensity factor with crack extension until for a certain crack extension, a saturation value, the corresponding critical long crack fracture toughness value, is reached.

Dislocation and twin shielding, crack bridging and shear ligaments, crack deflection and crack branching are the essential toughening mechanisms compared to ideal brittle failure. Dislocation and twin shielding are significant to enhance the initial crack propagation resistance. In contrast, crack bridging and shear ligaments, crack deflection and crack branching are the dominant contributions to enhance the crack extension dependent part of the crack growth resistance and finally the long crack fracture toughness. However, shielding by dislocation and twinning can also further increase. These contributions to the fracture toughness are present in all technical TiAl alloys, but to very different extents. As described, a clear separation of the individual contributions to fracture resistance is difficult; however, the discussed mechanisms can be used in the design of more damage-tolerant TiAl microstructures.

Fracture toughness is only one parameter in the strategy of alloy development. In addition, creep resistance in the temperature window between 450 and 750°C, the strength between room temperature and 750°C, and the minimum ductility in a tension experiment are equally or sometimes even more important. Additionally, fatigue and fatigue crack propagation are essential characteristics. Designed fully lamellar microstructures are excellent in respect of creep properties, and would be superb in respect of fracture toughness. For the latter, a very coarse colony size would be beneficial,[23] because it can increase the spreading of the crack and significantly enhance the crack bridging capacity. However, ideal or nearly ideal designed fully lamellar microstructures suffer from low ductility in tension, which is even more pronounced in coarse versions, because the first decohesion of a large colony will result in fatal failure of tension samples. Hence, new types of alloys (second and third generation of TiAl alloys) are based on a lamellar design, but with various well-designed phases at the colony boundaries.[24,25] This enhances ductility in even very high strength variants, but with an according reduction in fracture toughness. The key development of improved microstructures is usually not the improvement of a single property, such as the fracture toughness, which would be achieved by maximizing the individual described contributions, but the challenge rather lies in obtaining a balance of properties.

Funding

Open access funding provided by Montanuniversität Leoben.

Conflict of interest

On behalf of all authors, the corresponding author states that there is no conflict of interest.

Open access

References

1. A.A. Griffith, *Philos. Trans. R. Soc. Lond. A: Math. Phys. Eng. Sci.* **221**, 163 (1921)
2. R.O. Ritchie, *Mater. Sci. Eng.* **103**, 15 (1988)
3. J.J. Kruzic, J.P. Campbell, R.O. Ritchie, *Acta Mater.* **47**, 801 (1999)
4. S.J. Balsone, J.M. Larsen, D.C. Maxwell, J. Wayne Jones, *Mater. Sci. Eng. A* **192–193**, 457 (1995)
5. K.T.V. Rao, Y.-W. Kim, R.O. Ritchie, *Scr. Metall. Mater.* **33**, 459 (1995)
6. K.T. Venkateswara Rao, R.O. Ritchie, *Acta Mater.* **46**, 4167 (1998)
7. S.J. Zhu, L.M. Peng, T. Moriya, Y. Mutoh, *Mater. Sci. Eng. A* **290**, 198 (2000)
8. J.M. Larsen, B.D. Worth, S.J. Balsone, J.W. Jones, in *Gamma Titanium Aluminides*, Y.-W. Kim, R. Wagner, M. Yamaguchi, Eds. (The Minerals, Metals & Materials Society, Warrendale, PA, 1995), p. 821
9. E. Orowan, in *Fatigue and Fracture of Metals* (A Symposium held at the Massachusetts Institute of Technology, June 19–22, 1950) (Wiley, New York, 1952), p. 139
10. G.R. Irwin, *Trans. ASME Ser. E J. Appl. Mech.* **24**, 361 (1957)
11. M. Schloffer, A. Themeßl, E. Schwaighofer, H. Clemens, F. Heutling, D. Helm, M. Achtermann, S. Mayer, *4th International Workshop on Titanium Aluminides* (Nuremberg, Germany, September 13–16, 2011)
12. N. Saunders, in *Gamma Titanium Aluminides 1999,* Y.-W. Kim, D.M. Dimiduk, M.H. Loretto, Eds. (The Minerals, Metals & Materials Society, Warrendale, PA,1999), p. 183
13. T. Nakano, T. Kawanaka, H.Y. Yasuda, Y. Umakoshi, *Mater. Sci. Eng. A* **194**, 43 (1995)
14. R. Pippan, M. Höck, A. Tesch, C. Motz, M. Beschliesser, H. Kestler, in *Gamma Titanium Aluminides 2003*, Y.-W. Kim, H. Clemens, A.H. Rosenberger, Eds. (The Minerlas, Metals & Materials Society, Warrendale, PA, 2003), p. 521
15. T. Hebesberger, R. Pippan, O. Kolednik, C.O.A. Semprimoschnig, *Pract. Metallogr.* **37**(6), 301 (2000)
16. A. Neogi, R. Janisch, *Acta Mater.* **227**, 117698 (2022)
17. M. Burtscher, M. Alfreider, K. Schmuck, H. Clemens, S. Mayer, D. Kiener, *J. Mater. Res.* **36**, 2465 (2021)
18. J. Stampfl, O. Kolednik, *Int. J. Fract.* **101**, 321 (2000)
19. R. Pippan, *Eng. Fract. Mech.* **31**, 715 (1988)
20. B. Cotterell, J.R. Rice, *Int. J. Fract.* **16**, 155 (1980)
21. S.M. Ohr, *Mater. Sci. Eng.* **72**(1), 1 (1985)
22. G. Hénaff, A.-L. Gloanec, *Intermetallics* **13(**5), 543 (2005)
23. P. Wang, N. Bhate, K.S. Chan, K.S. Kumar, *Acta Mater.* **51**, 1573 (2003)
24 S. Mayer, P. Erdely, F.D. Fischer, D. Holec, M. Kastenhuber, T. Klein, H. Clemens, *Adv. Eng. Mater.* **19**, 1600735 (2017)
25. Y.-W. Kim, S.-L. Kim, *JOM* **70**, 553 (2018)

R. Pippan is currently a freelancer at the Erich Schmid Institute, Austria. His scientific career is mainly connected with the Erich Schmid Institute of the Austrian Academy of Sciences. His research activities are focused on mechanical properties of metals, alloys, and composites. The improvement of the basic understanding of the relations between the mechanical behavior, the deformation processes, the fracture processes, and the micro- and nanostructure of the material is his aim. The activities with respect to the properties can be separated into three groups: plastic deformation, fatigue and fracture, and micro- and nanomechanics. Pippan can be reached by email at reinhard.pippan@oeaw.ac.at.

A. Hohenwarter is a senior research assistant in the Department of Materials Science, Chair of Materials Physics at the University of Leoben, Austria. He studied materials science at the University of Leoben. His research interests concern mainly the fracture and fatigue behavior of ultrafine-grained and nanocrystalline metals and alloys. Hohenwarter can be reached by email at anton.hohenwarter@unileoben.ac.at.